2662 *Chem. Mater.* **2010,** *22,* 2662–2667
DOI:10.1021/cm100228d

CHEMISTRY OF MATERIALS
Article

# Synthesis of monodispersed $SnO_2$ nanocrystals and their remarkably high sensitivity to volatile organic compounds

Tetsuya Kida,*,† Takayuki Doi,‡ and Kengo Shimanoe†

†*Department of Energy and Material Sciences, Faculty of Engineering Sciences, Kyushu University, Kasuga-koen, Kasuga, Fukuoka, 816-8580, Japan, and* ‡*Innovative Collaboration Center, Kyoto University, Katsura Campus, Nishikyo-ku, Kyoto 615-8510, Japan*

*Received January 25, 2010. Revised Manuscript Received February 27, 2010*

In situ detection of volatile organic compounds (VOCs) in the atmosphere has become particularly important because of their detrimental effects on human health and the environment. To develop high-performance gas sensors capable of detecting VOCs in ppb concentrations, we prepared $SnO_2$ nanocrystals by a liquid-phase synthesis method. Nearly monodispersed $SnO_2$ nanocrystals (ca. 3.5 nm) were prepared by heating tin(IV) acetylacetonate in dibenzyl ether in the presence of oleic acid and oleylamine at 280 °C. The prepared nanocrystals exhibited high thermal stability against crystal growth, even at 600 °C, allowing for the fabrication of nanoparticulate gas-sensing films. The sensor device using the nanocrystals calcined at 600 °C exhibited significantly high sensor responses to VOCs such as ethanol, formaldehyde, and toluene at low ppm concentrations.

## Introduction

The synthesis of monodispersed nanocrystals has long been of scientific and technological importance. Recent advances in the synthesis methods allow for controlling the particle size and shape in the nanometer size range.[1] In particular, liquid-phase synthesis in high-boiling coordinating organic solvents using organometallic compounds or metal−surfactant complexes as precursors has been used successful for the synthesis of monodispersed nanocrystals. This method, which is based on the pioneering work of Bawendi et al.[2] and Alivisatos et al.,[3] has been modified and improved by a large number of researchers over the past decade[4] to synthesize monodispersed nanocrystals of metals, alloys, semiconductors, and oxides. Special attention has recently been paid to the synthesis of oxide nanocrystals because of their versatile functionalities for applications such as in catalysis, batteries, solar cells, and sensors. Thus, it is important to further develop these liquid-phase methods for the synthesis of a wide variety of oxide nanocrystals.

Tin oxide ($SnO_2$) has been investigated for its potential as a gas sensor material because of its high gas sensitivity, good stability, and low cost.[5] The sensing mechanism of $SnO_2$-based gas sensors relies on the diffusion of target gas molecules, such as $H_2$ and CO, into the sensing layer through its pores and their reaction with adsorbed oxygen on $SnO_2$. The removal of adsorbed oxygen molecules, upon interaction with combustible gases, leads to a decrease in the electric resistance of the sensor devices because adsorbed oxygen induces electron depletion on the surface of $SnO_2$. Such a change in the electrical resistance is utilized as the sensor signal (sensor response). Extensive studies have revealed some critical factors that govern the gas-sensing properties of $SnO_2$. Specifically, the following three factors have been proposed as being the most influential: crystalline size,[6] microstructure,[7]

*Corresponding author phone: +81-92-586-7537; fax: +81-92-586-7538; e-mail: kida@mm.kyushu-u.ac.jp.

(1) (a) Xia, Y.; Yang, P.; Sun, Y.; Wu, Y.; Mayers, B.; Gates, B.; Yin, Y.; Kim, F.; Yan, H. *Adv. Mater.* **2003**, *5*, 353. (b) Yin, Y.; Alivisatos, A. P. *Nature* **2005**, *437*, 664. (c) Park, J.; Joo, J.; Kwon, S. G.; Jang, Y.; Hyeon, T. *Angew. Chem., Int. Ed.* **2007**, *46*, 4630. (d) Tao, A. R.; Habas, S.; Yang, P. *Small* **2008**, *4*, 310.
(2) Murray, C. B.; Norris, D. J.; Bawendi, M. G. *J. Am. Chem. Soc.* **1993**, *115*, 8706.
(3) Bowen Katari, J. E.; Colvin, V. L.; Alivisatos, A. P. *J. Phys. Chem.* **1994**, *98*, 4109.
(4) (a) Peng, X.; Wickham, J.; Alivisatos, A. P. *J. Am. Chem. Soc.* **1998**, *120*, 5343. (b) Sun, S.; Murray, C. B.; Weller, D.; Folks, L.; Moser, A. *Science* **2000**, *287*, 1989. (c) Hyeon, T.; Lee, S. S.; Park, J.; Chung, Y.; Bin Na, H. *J. Am. Chem. Soc.* **2001**, *123*, 12798. (d) O'Brien, S.; Brus, L.; Murray, C. B. *J. Am. Chem. Soc.* **2001**, *123*, 12085. (e) Sun, S.; Zeng, H. *J. Am. Chem. Soc.* **2002**, *124*, 8204. (f) Shevchenko, E. V.; Talapin, D. V.; Rogach, A. L.; Kornowski, A.; Haase, M.; Weller, H. *J. Am. Chem. Soc.* **2002**, *124*, 11480. (g) Yin, M.; O'Brien, S. *J. Am. Chem. Soc.* **2003**, *125*, 10180. (h) Kim, S. W.; Park, J.; Jang, Y.; Chung, Y.; Hwang, S.; Hyeon, T. *Nano Lett.* **2003**, *3*, 1289. (i) Nakamura, H.; Kato, W.; Uehara, M.; Nose, K.; Omata, T.; Otsuka-Yao-Matsuo, S.; Miyazaki, M.; Maeda, H. *Chem. Mater.* **2006**, *18*, 3330. (j) Teranishi, T.; Saruyama, M.; Nakaya, M.; Kanehara, M. *Angew. Chem., Int. Ed.* **2007**, *46*, 1713.
(5) (a) Yamazoe, N. *Sens. Actuators: B* **1991**, *5*, 7. (b) Shimizu, Y.; Egashira, M. *MRS Bull.* **1999**, *24*, 18. (c) Yamazoe, N.; Sakai, G.; Shimanoe, K. *Catalysis Surveys from Asia* **2003**, *7*, 63. (d) Franke, M. E.; Koplin, T. J.; Simon, U. *Small* **2006**, *2*, 36. (e) Tiemann, M. *Chem.—Eur. J.* **2007**, *13*, 837.
(6) (a) Xu, C.; Tamaki, J.; Miura, N.; Yamazoe, N. *Sens. Actuators B* **1991**, *3*, 147. (b) Yamazoe, N.; Shimanoe, K. *J. Electrochem. Soc.* **2008**, *155*, J85–J92. (c) Yamazoe, N.; Shimanoe, K. *J. Electrochem. Soc.* **2008**, *155*, J93–J98.
(7) (a) Williams, D. E.; Henshaw, G. S.; Pratt, K. F. E.; Peat, R. *J Chem. Soc., Faraday Trans.* **1995**, *91*, 4299. (b) Shimizu, Y.; Maekawa, T.; Nakamura, Y.; Egashira, M. *Sens. Actuators B, Chem.* **1998**, *46*, 163. (c) Sakai, G.; Baik, N. S.; Miura, N.; Yamazoe, N. *Sens. Actuators B, Chem.* **2001**, *77*, 116.


Published on Web 03/12/2010

and surface modification (noble metal loading).[8] Among these, decreasing the crystalline size of $SnO_2$ is quite effective in improving its gas sensitivity; Xu et al. reported that the sensor response drastically increased as the crystal size decreased to less than 6 nm, which is twice as large as the thickness of the depletion layers in $SnO_2$.[6a] When the thickness of the depletion layers becomes comparable to the crystal radius, electron depletion layers form over the crystals, significantly increasing the difference in the electric resistance between in air ($O_2$) and in target gases. Many attempts have been made to improve the sensor performance by using nanocrystalline $SnO_2$.[9] We previously reported the preparation of $SnO_2$ nanocrystals by a hydrothermal method and showed that they exhibit high sensor responses to hydrogen.[9c]

Recently, the detection of volatile organic compounds (VOCs) using solid-state gas sensors has become particularly important because of their negative impacts on the environment and human health. However, their concentrations in the atmosphere are generally very low (below the ppm level) and thus are difficult to detect with conventional gas sensors. Consequently, the development of highly sensitive sensors is needed for the in situ detection of VOCs. In this study, to enhance the performance of $SnO_2$-based sensors for VOC detection, we prepared monodispersed $SnO_2$ nanocrystals by thermal decomposition of tin acetylacetonate in an organic solution with a high boiling point. Thermal decomposition of a tin−organic complex in an organic solution has already been reported to produce $SnO_2$ nanocrystals.[10] Based on recent theoretical considerations,[6b,6c] we anticipated that spherical $SnO_2$ nanocrystals with a narrow size distribution would exhibit improved gas sensing properties due to the effective formation of electron depletion layers in $SnO_2$ nanocrystals. Notably, the method can produce nanocrystals capped with organic surfactants, thereby making the nanocrystals soluble in organic solvents. This feature allows for the straightforward fabrication of gas-sensing films by a simple coating method using an organic solvent-based suspension containing nanocrystals.

## Experimental Section

**Materials.** Tin(IV) acetylacetonate dichloride was purchased from Aldrich. Trimethylamine-*N* oxide was purchased from Tokyo Chemical Industry. Dibenzyl ether, oleylamine, olyeic acid, hexane, ethanol, and pyridine were purchased from Kishida Chemical. All chemicals were used as received.

**Material Preparation and Evaluation.** In a three-neck flask (100 mL), tin(IV) acetylacetonate dichloride (0.4 mmol) was mixed with dibenzyl ether (7 mL) containing oleylamine (0.6 mL) and olyeic acid (0.6 mL) as capping agents. The solution was heated at 140 °C for 1 h in air. Then, trimethylamine-*N* oxide was added to the solution under a $N_2$ flow in a glovebox. The solution was reheated at 140 °C for 1 h in $N_2$, and then further heated at 280 °C to reflux for 30 min, producing a brown suspension. Ethanol was added to the suspension to precipitate the particles after the suspension was cooled to room temperature. The particles were recovered from the suspension by centrifugation at 6000 rpm for 10 min. The particles were dispersed in hexane, mixed with ethanol, and centrifuged again. This treatment was repeated three times in order to purify the product. Finally, the particles were dissolved in hexane.

The particles were recollected from the hexane suspension by centrifugation, mixed with pyridine (10 mL), and heated at 110 °C to reflux for 12 h under a $N_2$ flow. After heat treatment, hexane was added to the solution to precipitate the particles. The particles were recovered from the pyridine suspension by centrifugation at 6000 rpm for 10 min. The particles were dispersed in tetrahydrofuran (THF), mixed with hexane, and centrifuged again. This treatment was repeated three times in order to purify the particles. Finally, the particles were recovered by centrifugation and then redispersed in THF to form a stable suspension.

The particles were analyzed by X-ray diffractmetry using Cu Kα radiation (XRD; RINT2100, Rigaku), transmission electron microscopy (TEM; JEM2100F, JEOL), field emission-scanning electron microscopy (FE-SEM; S-4800, Hitachi High-Technologies), Fourier transform infrared spectrometry (FT-IR; 4100, JASCO) and thermogravimetry/differential thermal analysis (TG-DTA; EXSTAR 6000, Seiko Instruments).

**Sensor Fabrication and Sensing Measurements.** Sensor devices were fabricated by casting drops of the obtained THF suspension on alumina substrates ($9 \times 13 \times 0.38$ mm) equipped with a pair of comb-type Au microelectrodes (line width: 180 $\mu$m; distance between lines: 90 $\mu$m; sensing layer area: 64 $mm^2$). The casting and drying procedure was repeated five times to produce sensing films with ca. 7 $\mu$m thickness. The surfaces of the alumina substrates were treated with an ammonia solution containing hydrogen peroxide at 80 °C and then subjected to plasma cleaning (PS-601S, KASUGA ELECTRIC) prior to use. The Au electrodes were fabricated by screen-printing using a commercial Au paste, followed by calcination at 850 °C just before sensing film deposition. Then, the sensing films deposited on the substrates were calcined at 600 °C for 3 h in air. The morphology of the sensing films was observed with FE-SEM and atomic force microscopy (AFM; SPM-9600, SHIMADZU).

(8) (a) Matsushima, S.; Maekawa, T.; Tamaki, J.; Miura, N.; Yamazoe, N. *Chem. Lett.* **1989**, *18*, 845. (b) Kappler, J.; Bârsan, N.; Weimar, U.; Dièguez, A.; Alay, J. L.; Romano-Rodriguez, A.; Morante, J. R.; Göpel, W. *Freseniuś J. Anal. Chem.* **1998**, *361*, 110. (c) Epifani, M.; Arbiol, J.; Pellice, E.; Comini, E.; Sicilian, P.; Faglia, G.; Morante, J. R. *Cryst. Growth Des.* **2008**, *8*, 1774.
(9) (a) Ansaria, S. G.; Boroojerdiana, P.; Sainkarb, S. R.; Karekara, R. N.; Aiyera, R. C.; Kulkarnia, S. K. *Thin Solid Films* **1997**, *295*, 271. (b) Nayral, C.; Viala, E.; Fau, P.; Senocq, F.; Jumas, J. C.; Maisonnat, A.; Chaudret, B. *Chem.—Eur. J.* **2000**, *6*, 4082. (c) Baik, N. S.; Sakai, G.; Shimanoe, K.; Miura, N.; Yamazoe, N. *Sens. Actuators B, Chem.* **2000**, *65*, 97. (d) Epifani, M.; Prades, J. D.; Comini, E.; Pellicer, E.; Avella, M.; Siciliano, P.; Faglia, G.; Cirera, A.; Scotti, R.; Morazzoni, F.; Morante, J. R. *J. Phys. Chem. C* **2008**, *112*, 19540.
(10) Epifani, M.; Arbiol, J.; Díaz, R.; Perálvarez, M. J.; Siciliano, P.; Morante, J. R. *Chem. Mater.* **2005**, *17*, 6468.

The VOC-sensing properties of the devices were examined using a conventional gas flow apparatus equipped with an electric furnace at a gas flow rate of 100 $cm^3$/min. The flow rates of air and the sample gases were precisely controlled by mass flow controllers (SEC-series; HORIBA STEC). The sample gases of toluene, formaldehyde, and ethanol in air were prepared by diluting parent synthetic gas mixtures with synthetic air. The parent synthetic gas mixtures were purchased from Sumitomo Seika Chemicals. Each sensor device was connected with a standard resistor in series, and the voltage across the standard resistor was measured under an applied voltage of DC 4 V to evaluate the electrical resistance of the devices. The electrical signal of the sensor was acquired with an electrometer (TR2114; Advantest). The sensor response ($S$) was defined as the ratio of resistance in air ($R_a$) to that in air containing VOC gases ($R_g$) ($S = R_a/R_g$).

## Results and Discussion

Figure 1 (a) shows the X-ray diffraction (XRD) pattern of $SnO_2$ nanocrystals prepared by heating tin acetylacetonate in dibenzyl ether in the presence of oleylamine and oleic acid at 280 °C. The pattern matches that of tetragonal $SnO_2$ (JCPDS: 41−1445), and the broad peaks are indicative of the formation of nanosized $SnO_2$ crystals. Furthermore, the synthesized crystals displayed excellent thermal stability; the peak widths did not significantly decrease even after calcination at 600 °C, as shown in Figure 1 (b). Sensing films are usually fabricated by calcination at elevated temperatures to firmly attach the films onto substrates, but this also induces particle growth and particle sintering. Thus, thermal resistance against particle growth is preferable for fabricating nanoparticulate gas-sensing films with well-distributed pores. The FT-IR measurements confirmed the presence of oleic acid (or its moieties formed by decomposition) on the surface of $SnO_2$ nanocrystals, as shown in Supporting Information (SI) Figure S1(a). Oleic acid firmly attached on the surface and was not completely removed by calcination at 600 °C (see SI Figure S1(b)). Thus, the adsorbed organic capping agents possibly prevented particle growth. The presence of organic compounds on the as-prepared nanocrystals was also confirmed by TG-DTA analysis, which showed a weight loss of about 20% after calcination at 600 °C (see SI Figure S2).

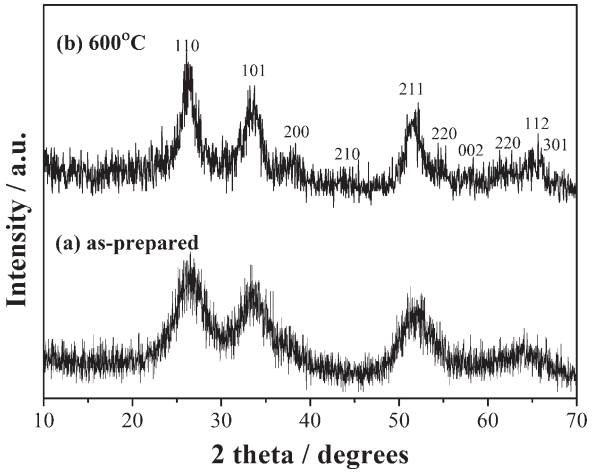


**Figure 1.** XRD patterns of (a) $SnO_2$ nanocrystals prepared by thermal decomposition of Tin(IV) acetylacetonate dichloride in dibenzyl ether at 280 °C and (b) after calcination at 600 °C for 3 h.

The synthesized $SnO_2$ nanocrystals were soluble in nonpolar solvents such as hexane and benzene. However, the stability of the suspensions was poor; sedimentation of the crystals occurred after the suspensions were left for 1 or 2 days. On the other hand, treatment of the surface with pyridine rendered the nanocrystals soluble in polar organic solvents such as 2-propanol and THF. Pyridine treatment yielded a very stable suspension ideal for making gas-sensing films. The presence of pyridine on the surface was confirmed by FT-IR analysis (see SI Figure S1 (c)). The inset of Figure 2 (a) shows a photograph of a THF suspension containing $SnO_2$ nanocrystals treated with pyridine. The color of the suspension is brown, which is different from the white color of a typical $SnO_2$

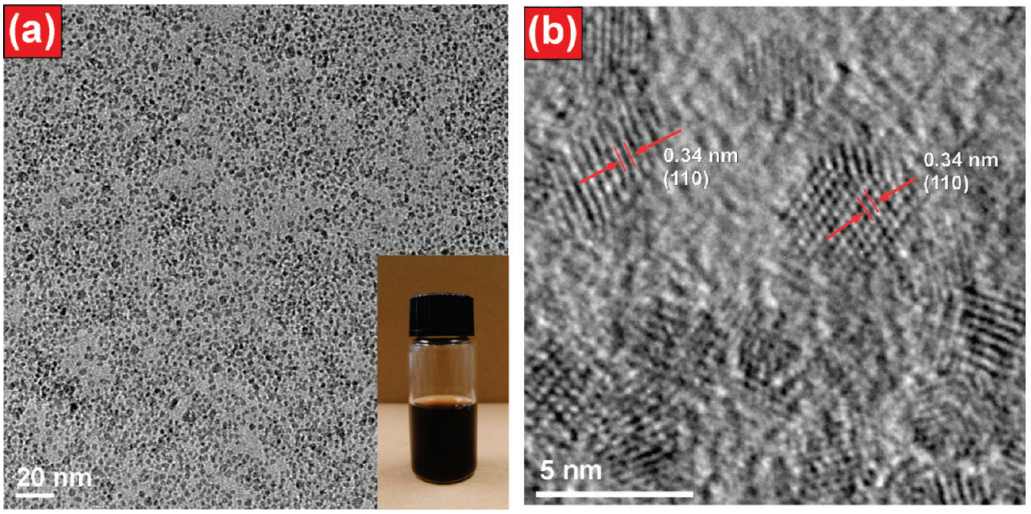


**Figure 2.** TEM images of $SnO_2$ nanocrystals treated with pyridine: (a) low and (b) high magnification images. The inset shows a photograph of a THF suspension containing $SnO_2$ nanocrystals treated with pyridine. A drop of the suspension was directly deposited on a copper grid for observation by TEM.

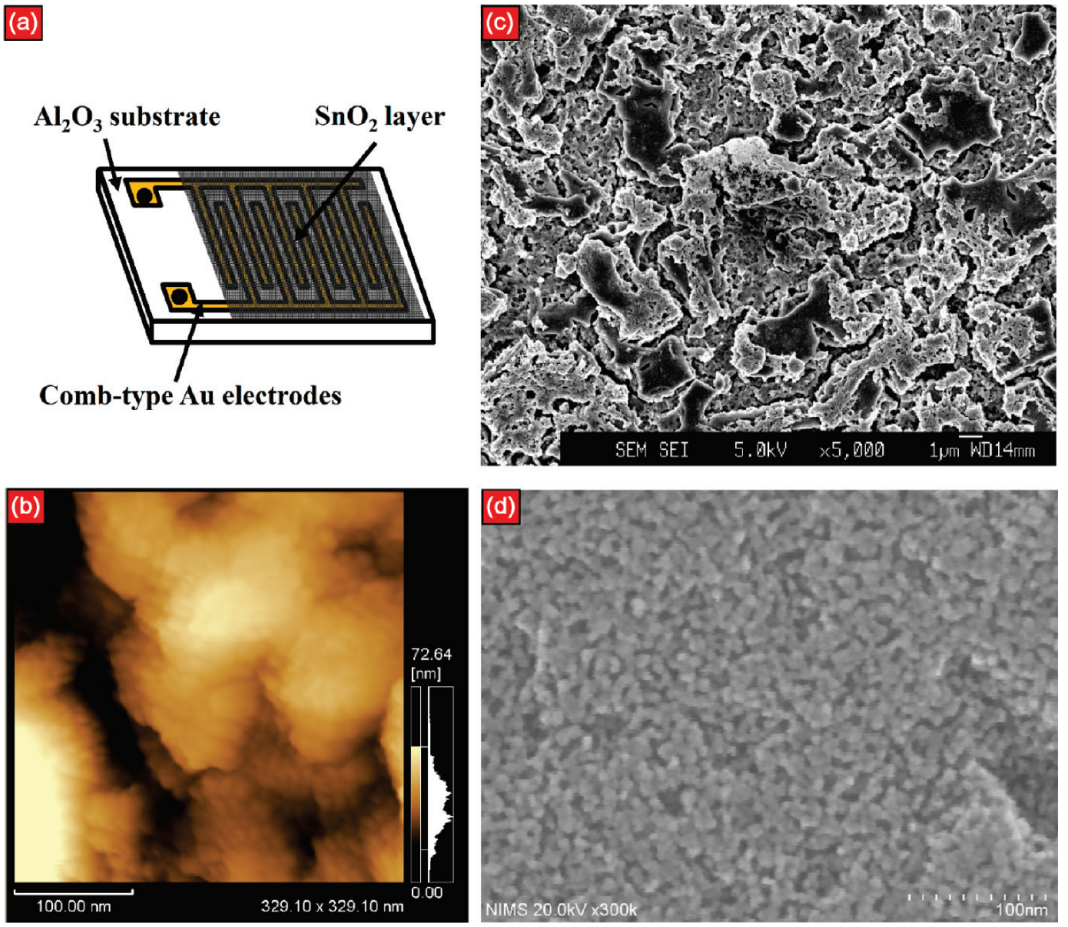


**Figure 3.** Schematic structure of a gas sensor device and microstructures of a sensing layer deposited using a THF suspension: (a) device structure, (b) AFM image, and (c) lower and (d) higher magnifications of SEM images of the sensing layer after calcination at 600 °C.

suspension. This suggests the presence of moieties of the organic precursors resulting from pyrolysis on the surface together with oleic acid and pyridine. Figures 2 (a) and (b) display TEM images of $SnO_2$ nanocrystals after pyridine treatment. The synthesized nanocrystals were well dispersed without agglomeration. Furthermore, they exhibited good crystallinity; the lattice spacing closely corresponded to that of the {110} plane of $SnO_2$, as shown in Figure 2 (b). The crystals were nearly monodispersed and their average size was estimated to be 3.5 nm.

Figure 3 (a) shows the structure of the fabricated gas sensor device. The $SnO_2$ nanocrystals were deposited on an alumina substrate by casting of a THF suspension, thereby forming a sensing layer with a thickness of ca. 7 $\mu$m. As shown in the AFM and SEM images (Figure 3 (b)−(d)), the sensing film had a rough and porous morphology with randomly distributed surface macropores. No significant crystal growth occurred and the size of the crystals remained small (ca. 9 nm) even after high-temperature calcination at 600 °C. The suppression of particle sintering yielded mesopores for efficient gas diffusion even in agglomerated regions, as seen in the SEM image (Figure 3 (c)).

Figure 4 shows the gas-sensing properties of the fabricated device to hydrogen, CO, and VOCs. Hydrogen and CO were used as probe gases to examine the basic gas-sensing properties of the device. The device exhibited high sensor responses to hydrogen and CO (200−1000 ppm) at 300−400 °C, as shown in Figure 4 (a) and (b). This suggests that any remaining organic compounds on the nanocrystal surface had no significant adverse effects on the sensor response. We also confirmed that the present film fabrication method using the nanocrystal suspension can produce highly sensitive films with good reproducibility. The sensor responses ($S = R_a/R_g$) monotonically decreased with an increase in the operating temperature, although the response and recovery speeds had the opposite trend. Thus, the operating temperature was set to 350 °C to balance the sensor response and the response-recovery speeds. The device provided significantly high sensor responses to typical VOCs, such as toluene, formaldehyde, and ethanol, in ppm ranges at 350 °C; for example, a sensor response exceeding 1000 (three-orders of magnitude change in the resistance) was achieved for 50 ppm ethanol, as shown in Figure 4 (c). These sensor responses to VOCs are much larger than those reported for other metal oxide-based gas sensors,[11]

(11) (a) Yu, Q.; Yu, C.; Fu, W.; Yuan, M.; Guo, J.; Li, M.; Liu, S.; Zou, G.; Yang, H. *J. Phys. Chem. C* **2009**, *113*, 12016. (b) Jia, Y.; He, L.; Guo, Z.; Chen, X.; Meng, F.; Luo, T.; Li, M.; Liu, J. *J. Phys. Chem. C* **2009**, *113*, 9581. (c) Cao, M.; Wang, Y.; Chen, T.; Antonietti, M.; Niederberger, M. *Chem. Mater.* **2008**, *20*, 5781. (d) Chiu, H. C.; Yeh, C. S. *J. Phys. Chem. C* **2007**, *111*, 7256.

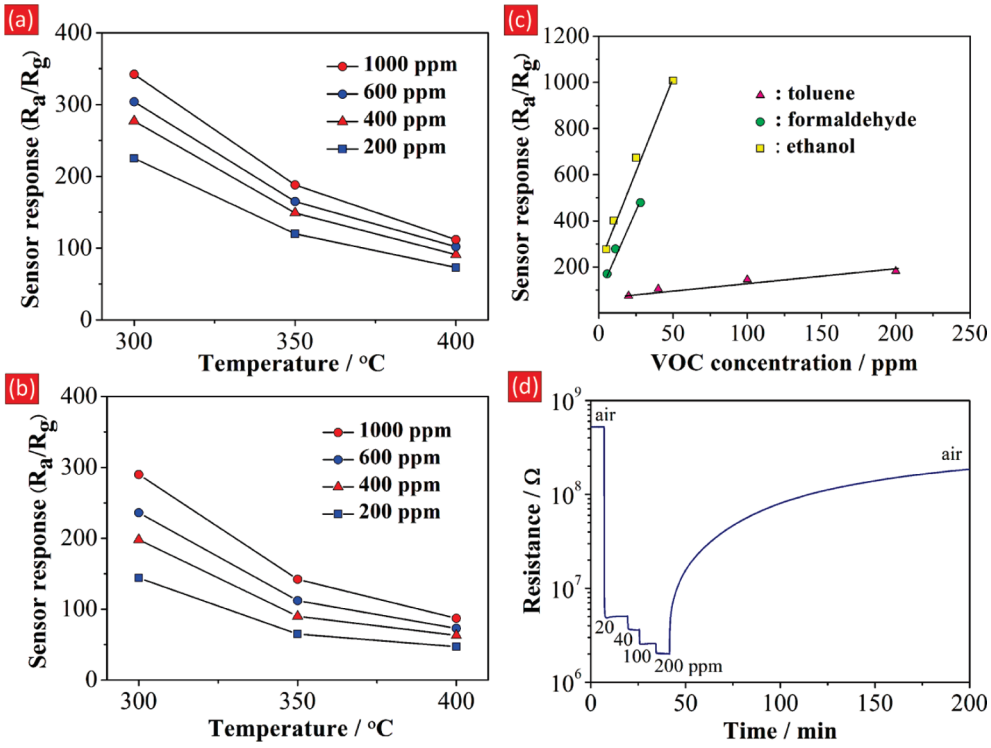


**Figure 4.** Gas-sensing properties of the sensor device using $SnO_2$ nanocrystals deposited on an alumina substrate after calcination at 600 °C. Sensor responses to (a) hydrogen and (b) CO (200−1000 ppm) as a function of temperature; (c) Dependence of the sensor responses on VOC concentrations at 350 °C. (d) Transient response of the device to toluene (20−200 ppm) at 350 °C.

although the experimental conditions were different. In addition, the detection limits for each gas, roughly estimated from the extrapolated dependence of the sensor response on concentration, are below 2 ppb (see SI Figure S3). Notably, the fabricated sensing film was packed with nanocrystals (ca. 9 nm) without significant particle sintering, as revealed by SEM and AFM. Thus, the surface and the bulk of the nanocrystals can be electrically depleted upon oxygen adsorption, thereby increasing the magnitude of an electrical resistance change upon interaction of the nanocrystals with combustible gases. As suggested by the SEM results (Figure 3 (d)), there were many mesopores of around 10 nm in the regions with closely packed crystals. Experimental and theoretical evidence suggests that the pore size (porosity) of sensing films greatly influences their gas-sensing behaviors, particularly for larger sized gases.[12] Thus, the observed nanoporous structure is likely to facilitate the diffusion of large VOCs deep inside the film and improve the sensor response. The lower diffusivity and reactivity of toluene may account for the lower sensor responses to toluene among the VOCs tested. The device can selectively detect ethanol and formaldehyde without significant interference of $H_2$ and CO with lower concentrations, due to its higher sensitivity to VOCs. It is expected that the high sensitivity of the film to combustible gases would also effectively suppress the interference from humidity, which is known to affect the sensitivity of $SnO_2$-based gas sensors.[13] The device also showed a good response speed, although the recovery was rather slow, as shown in Figure 4 (d). Slow desorption of VOCs from the sensing layer at 350 °C may retard the recovery of the resistance to the original value in air. Optimization of either the operating temperature or the material design (such as loading of foreign elements) would improve the recovery speed.

## Conclusion

Nearly monodispersed $SnO_2$ nanocrystals with ca. 3.5 nm were prepared by heating tin acetylacetonate in dibenzyl ether at 280 °C. The treatment of the nanocrystals with pyridine provided a stable THF-based suspension, which was used to deposit a nanoparticulate film on an alumina substrate. The nanocrsytals showed high thermal stability against particle growth, even at the sensor fabrication temperature of 600 °C. The sensing film packed with nanocrsytals (ca. 9 nm) exhibited significantly high sensor responses to VOCs (5−200 ppm), such as ethanol, formaldehyde, and toluene, at the operating temperature of 350 °C. Because of its high sensitivity, the fabricated sensor device is potentially applicable for the in situ detection of VOCs in ppb ranges.

**Acknowledgment.** This work was supported by a research grant from the Iketani Science and Technology Foundation, an environmental research and technology development

(12) (a) Sakai, G.; Matsunaga, N.; Shimanoe, K.; Yamazoe, N. *Sens. Actuators B, Chem.* **2001**, *80*, 125. (b) Vuong, D. D.; Sakai, G.; Shimanoe, K.; Yamazoe, N. *Sens. Actuators B, Chem.* **2005**, *105*, 437. (c) Seo, M.-H.; Yuasa, M.; Kida, T.; Huh, J.-S.; Shimanoe, K.; Yamazoe, N. *Sens. Actuators B, Chem.* **2009**, *137*, 513.

(13) (a) Bârsan, N.; Weimar, U. *J. Phys. Condens. Matter.* **2003**, *15*, R813. (b) Capone, S.; Siciliano, P.; Quaranta, F.; Rella, R.; Epifani, M.; Vasanelli, L. *Sens. Actuators B, Chem.* **2001**, *77*, 503.

fund from the Ministry of Environment of Japan, and a research grant for promoting technological seeds from the Japan Science and Technology Agency (JST). We acknowledge support for the SEM measurements from the NIMS Center for Nanotechnology Network.

**Supporting Information Available:** FT-IR spectra and TG-DTA curves of the nanocrystals, and log−log dependence of sensor responses to VOCs on their concentrations (PDF). This material is available free of charge via the Internet at http://pubs.acs.org.